

Preparation and water adsorption property of a mesoporous TiO₂-montmorillonite nanocomposite

Yang-Su Han^a, Jae-Won Lee^b and Sun-Min Park^{b,*}

^aNanomaterials Laboratory, Nanospace Co.,Ltd. Ansan 425-839, KOREA

^bKorea Institute of Ceramic Engineering and Technology, 103 Fashion Danji-gil, Geumcheon -Gu, Seoul 153-801, KOREA

Nanocrystalline TiO₂ particles with a mean particle diameter of 5 nm and a positive surface charge were coagulated with delaminated silicate layers to form a heterocoagulated mesoporous nanocomposite. Nitrogen sorption isotherm analysis revealed the TiO₂-montmorillonite nanocomposite to have a specific surface area (S_{BET}) and pore volume (V_{tot}) of 253 m²/g and 0.36 mL/g, respectively. Water isotherm measurements also showed that the mesoporous nanocomposite has a large water sorption capacity of 0.37 ml/g and large adsorption-desorption hysteresis, which is suitable for self-humidity control materials.

Key words: Nanoparticle, TiO₂, Montmorillonite, Mesoporous materials, Water isotherm.

Introduction

In an attempt to improve the limited pore size range of zeolites, there has been increasing interest in the preparation of novel, two-dimensional molecular sieve-type materials based on clays, known as pillared interlayer clays (PILCs). [1-4] PILCs have attracted considerable attention as a new type of microporous solids that can serve as shape-selective catalysts, catalytic supports, separating agents, adsorbents, desiccation materials, etc.

These materials are usually prepared by ion-exchanging the cations in the interlayer region of the swelling clays with bulky metal polyoxycations and positively charged colloidal particles. The intercalated species can prevent the collapse of the interlayer spaces, propping open the layers as pillars, and forming an interlayer space, i.e., a two-dimensional porous network. Upon heating, the intercalated inorganic species are converted to metal oxide clusters, generating a stable microporous structure. Thus far various types of metal oxides have been used as pillars to maintain separation of the silicate layers [5-10].

Among many potential applications of PILCs, their use as humidity-controlling materials has attracted considerable attention on account of their large microporosity and tunable pore size. The water adsorption behavior on a series of Al-PILCS has been reported by Yamanaka *et al.* [11]. Malla and Kormarneni [12] extended the work to zirconia and titania pillared clays as well as to Al-PILC modified by Ca²⁺ cations. They reported that the water sorption capacity of pillared clays is comparable to those zeolites and silica gel. The influence of metal cation doping

in the pillared clays on the microporosity and water sorption behavior was studied systematically by Zhu *et al.* [13-15]. They found that the water sorption behavior is strongly affected by the porosity and surface properties of the pillared clays. This study prepared a new-type of mesoporous TiO₂-montmorillonite nanocomposite and characterized the water adsorption-desorption behavior.

Experimental

Materials

A commercially available aqueous titania sol solution (TS-50, Nanospace Co.,Ltd) was used as the TiO₂ pillaring agent. The TiO₂ particles had an anatase-type crystalline structure with an average particle size of ~5 nm. The pH of the colloidal solution was 1.5 and the solid content was 5 wt%. Natural Na-montmorillonite (Kunipia G, Kunimine Industry, Japan) with a chemical formula of Na_{0.35}K_{0.01}Ca_{0.02}(Si_{13.89}Al_{0.11})(Al_{1.60}Mg_{0.32}Fe_{0.08})O₁₀(OH)₂nH₂O and cation exchange capacity (CEC) of 100 mequiv./100 g was used as the host clay. An aqueous suspension (1 wt%) of the montmorillonite was prepared and pre-swelled for 24 h before the ion exchange reaction.

Preparation

The TiO₂-montmorillonite nanocomposite was prepared using the following procedure. Initially, a TiO₂ colloidal solution was diluted to 0.1 wt% TiO₂ by adding distilled water. The solution pH was then adjusted to 1.5 by adding a 0.1 N HCl solution dropwise. The positively charged TiO₂ sol particles prepared were then coagulated with the negatively charged clay layers. In a typical heterocoagulation experiment, a 0.1 wt% TiO₂ colloidal solution was added dropwise to a 1.0 wt% clay suspension under vigorous stirring. The mixing mole ratio of the Ti/CEC was fixed at 50/1. The heterocoagulated precipitate formed rapidly,

*Corresponding author:
Tel : +82-2-3282-2462
Fax: +82-2-3282-2475
E-mail: psm@kicet.re.kr

which was allowed to incubate at room temperature for 12 h. The precipitate was centrifuged, washed with thoroughly distilled water, dried at 70 °C for 24 h, and finally heat treated at 400 °C for 4 h under an ambient atmosphere.

Characterization

Transmission electron microscopy (TEM, JEOL-2020) was performed at an accelerating voltage of 200 kV. The powder X-ray diffraction (XRD, MXP3A-HF22, MAC Science Co.) patterns were obtained on the oriented samples using graphite monochromatized Cu K α radiation ($\lambda = 1.5405 \text{ \AA}$). The average crystallite size was calculated using the Scherrer equation. The nitrogen adsorption-desorption isotherms were measured on a Micrometric ASAP-2010 instrument using nitrogen at 77 K. Prior to the sorption measurements, the samples were degassed at 250 °C for 4 h under a reduced pressure ($< 1 \mu\text{Pa}$). The specific surface areas were estimated using the BET equation. The pore size distribution curves were also calculated based on the adsorption branches of the nitrogen isotherms using the BJH method [16]. Water adsorption-desorption isotherms were measured using a volumetric method on a BELSORP-18 (Bel Japan Inc.) instrument at 25 °C. Before the sorption measurements, the samples were preheated to 250 °C for 4 h under a vacuum.

Results and Discussion

The TEM images of the TiO₂ colloidal solutions clearly show the presence of TiO₂ nanoparticles (Fig. 1) with a mean particle diameter of $\sim 5 \text{ nm}$. The micrograph also indicates that the nanoparticles have reasonable monodispersity. The crystallite size of the nanoparticles, which was estimated from the broadening of the (101) titanium dioxide XRD peak at $25.4^\circ 2\theta$ (Fig. 2(b)), was 4.5 nm which is consistent with the TEM observations.

Fig. 2 shows the XRD patterns of (a) host montmorillonite, (b) TiO₂ nanoparticles, and (c) heterocoagulated nanocomposite heat treated at 400 °C, respectively. The pristine montmorillonite (a) and anatase-type TiO₂ nanoparticles (b) exhibited typical reflection profiles corresponding to

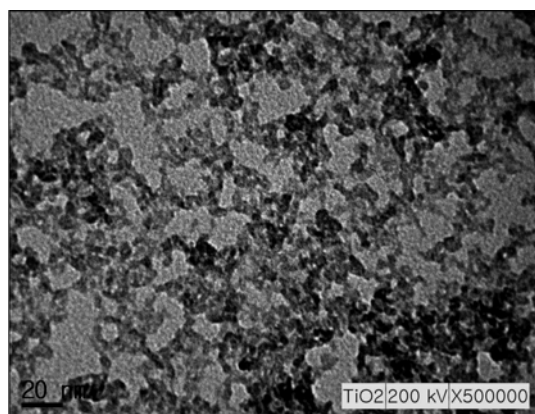


Fig. 1. TEM image of the TiO₂ nanoparticles.

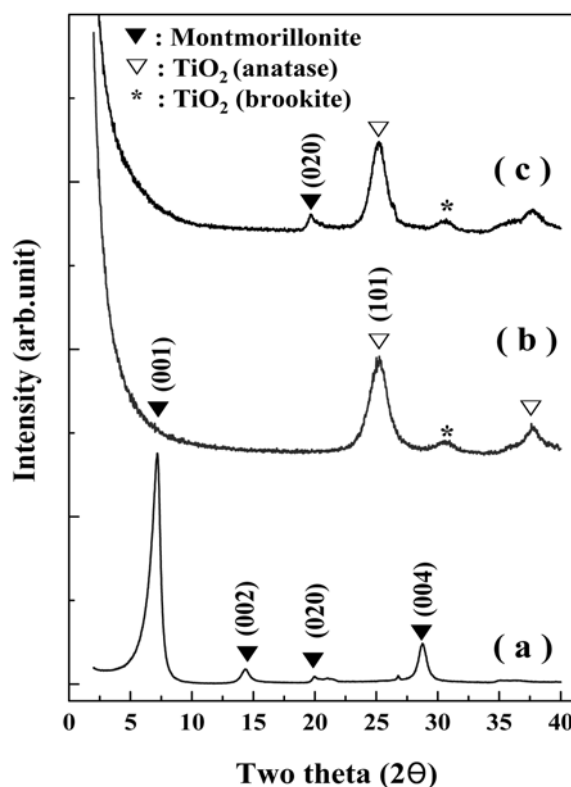


Fig. 2. XRD patterns of (a) pristine montmorillonite, (b) TiO₂ nanoparticles, and (c) TiO₂-montmorillonite nanocomposite calcined at 400 °C, respectively.

their crystalline phases, even though a trace amount of brookite phase was observed, as shown in Fig. 2(b). The heterocoagulated nanocomposite (c) did not show any reflections over the $1\sim 10^\circ (2\theta)$ range; only the presence of a small shoulder in the lower 2θ domain indicated the possibility of larger ($> 5 \text{ nm}$) pillars, or a turbostratic stacking structure of TiO₂ nanoparticles and delaminated silicate layers on the nanometre scale. It should be noted that the (020) reflection at $19.7^\circ 2\theta$ could be clearly observed in the heterocoagulated nanocomposite. This finding shows that the exfoliated clay particles are dispersed homogeneously in the nanocomposite, even though the ordered layer stacking structure collapsed.

The typical (101) TiO₂ reflection at $25.4^\circ 2\theta$ also shows the stabilization effect of montmorillonite, because the half-width values of the peaks (2.14° for the TiO₂ nanoparticles (b) and 2.11° for the nanocomposite (c)) do not change significantly after the pillaring and heating process, indicating the formation of TiO₂ nanoparticles with the same size. Therefore, the microstructure of the TiO₂-montmorillonite nanocomposite can be regarded as a turbostratic stacking structure of TiO₂ nanoparticles and delaminated clay particles, which is similar to that reported previously [17-19].

Fig. 3 compares the nitrogen adsorption-desorption isotherms for (a) pristine montmorillonite, (b) TiO₂ nanoparticles dried at 250 °C for 4 h, and (c) TiO₂-montmorillonite nanocomposite calcined at 400 °C for 4 h, respectively.

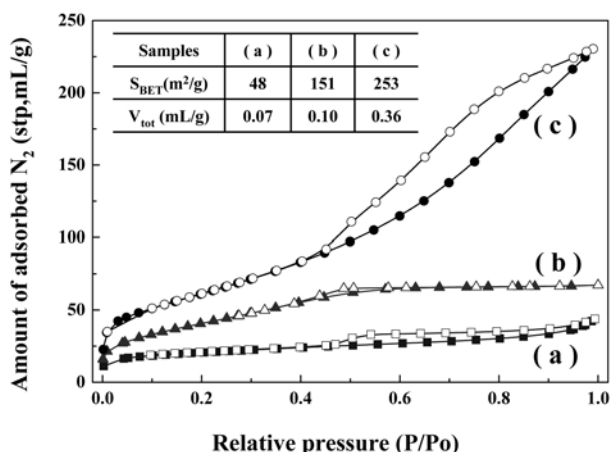


Fig. 3. N₂ adsorption-desorption isotherms and porous parameters (inset); (a) pristine montmorillonite, (b) TiO₂ nanoparticles dried at 250 °C, and (c) TiO₂-montmorillonite nanocomposite calcined at 400 °C, respectively.

The specific surface areas (S_{BET}) using the linearized BET equation are also summarized in the figure along with the total pore volumes (V_{tot}). The nitrogen adsorption isotherms in Fig. 3 showed that the porous structure and adsorption characteristics of montmorillonite were altered significantly by heterocoagulation with TiO₂ nanoparticles. The specific surface area ($S_{BET} = 253 \text{ m}^2/\text{g}$) and pore volume ($V_{tot} = 0.36 \text{ mL/g}$) of the nanocomposite were considerably higher than those of the pristine montmorillonite and TiO₂ nanoparticles. Although the nitrogen uptake in the nanocomposite was increased over the entire P/P₀ range, a much steeper increase in nitrogen uptake can be observed in the higher P/P₀ domain, indicating a greater contribution by mesopores than micropores. This suggests that a large number of mesopores are created by heterocoagulation between the TiO₂ particles and delaminated silicate layers, leading to a new type of mesoporous nanocomposite.

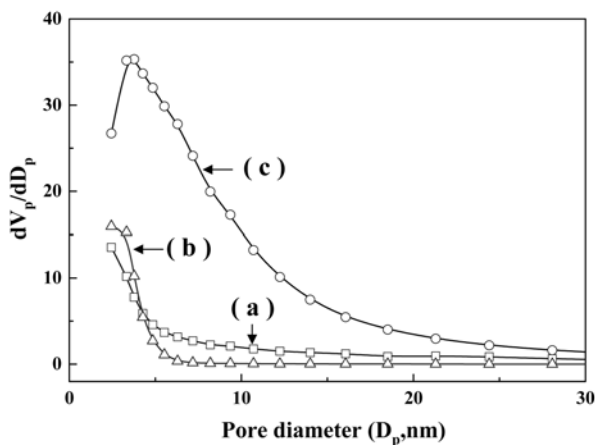


Fig. 4. Pore size distribution curves calculated by the BJH method using adsorption branches: (a) pristine montmorillonite, (b) TiO₂ nanoparticles dried at 250 °C, and (c) TiO₂-montmorillonite nanocomposite calcined at 400 °C, respectively. The distribution curves of (a) and (b) are enlarged by a factor of 10³ for comparison.

The pore size distribution curves (Fig. 4) also demonstrates that the nanocomposite contains a considerably large number of mesopores than the montmorillonite and TiO₂ nanoparticles. The nanocomposite sample exhibited a pore size distribution maximum at 3.5–4.0 nm, which were created mainly in the interstices between the TiO₂ nanoparticles and delaminated silicate layers.

Fig. 5 shows the water adsorption-desorption isotherms measured at 25 °C. Fig. 5(a) represents a sorption isotherm of pure montmorillonite. Both the adsorption and desorption isotherms exhibited stepwise hydration and dehydration, respectively, showing the typical swelling behavior of clay minerals. The TiO₂ nanoparticles (Fig. 5(b)) showed a relatively low water sorption capacity and the hysteresis loop could be characterized as type H2 in the IUPAC classification [20]. Some corpuscular systems (e.g. certain silica

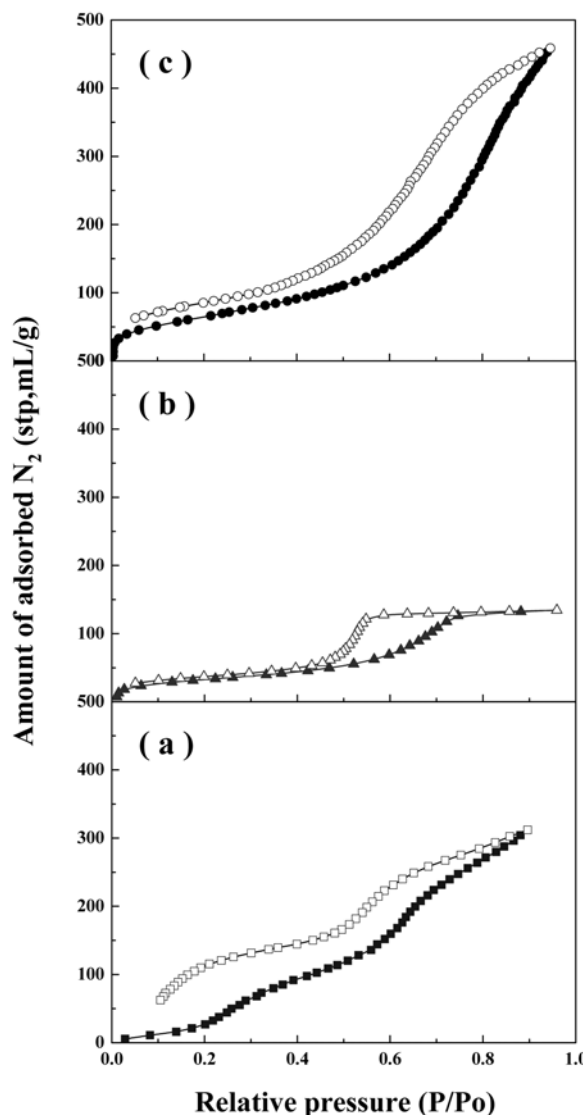


Fig. 5. Water adsorption-desorption isotherms measured at 25 °C; (a) pristine montmorillonite, (b) TiO₂ nanoparticles dried at 250 °C, and (c) TiO₂-montmorillonite nanocomposite calcined at 400 °C, respectively.

gels) tend to provide H2 loops, indicating that the aggregation of TiO₂ nanoparticles have a microporous structure like silica gels. The mesoporous TiO₂-montmorillonite nanocomposite (Fig. 5(c)) showed a significant water sorption capacity. The maximum sorption amount reached 0.38 ml/g (liquid). In the adsorption curve, the water uptake increased remarkably beyond P/Po = 0.6, suggesting the Kelvin capillary condensation of water molecules in the mesopores. The large hysteresis observed in the desorption branch can also be attributed to the capillary condensation effect in mesopores. The water isotherm hysteresis curve obtained in the TiO₂-montmorillonite nanocomposite is quite suitable for use as a self-humidity control material.

Conclusions

Mesoporous TiO₂-montmorillonite nanocomposites were prepared by heterocoagulation between positively charged TiO₂ nanoparticles and negatively charged delaminated clay layers. The mesoporous nanocomposite exhibited a high specific surface area ($S_{\text{BET}} = 253 \text{ m}^2/\text{g}$) and large pore volume ($V_{\text{tot}} = 0.36 \text{ ml/g}$), which were attributed mainly to the mesopores created in the interstices between the TiO₂ nanoparticles and silicate layers. Water sorption isotherm analysis showed that the TiO₂-montmorillonite mesoporous composite had a large water sorption capacity (0.37 ml/g) and large hysteresis during adsorption and desorption, which is suitable for use as a self-humidity controlling material.

References

1. R. Burch (Ed.), *Catal. Today*. 2[2-3] (1988) 185-186.

2. E.M. Serwicka and K. Bahranowski, *Catal. Today*. 90[1-2] (2004) 85-92.
3. K. Ohtsuka, *Chem. Mater.* 9[10] (1997) 2039-2050.
4. J.T. Kloproge, *J. Porous Mater.* 5[1] (1998) 5-11.
5. Y.S. Han, H. Matsumoto and S. Yamanaka, *Chem. Mater.* 9[9] (1997) 2013-2018.
6. Y.S. Han and S. Yamanaka, *J. Porous Mater.* 5[2] (1998) 111-119.
7. Y.S. Han and J.H. Choy, *J. Mater. Chem.* 8[6] (1998) 1459-1463.
8. Y.S. Han, S. Yamanaka and J.H. Choy, *Appl. Catal. A* 174[1-2] (1998) 83-90.
9. Y.S. Han, S. Yamanaka and J.H. Choy, *J. Solid State Chem.* 144[1] (1999) 45-52.
10. Y.S. Han and S. Yamanaka, *J. Solid State Chem.* 179[4] (2006) 1146-1153.
11. S. Yamanaka, P.B. Malla and S. Kormameni, *J. Colloid Inter. Sci.* 134[1] (1990) 51-58.
12. P.B. Malla and S. Kormameni, *Clays Clay Mineral.* 38[4] (1990) 363-372.
13. H.Y. Zhu, W.H. Gao and E.F. Vansant, *J. Colloid Inter. Sci.* 171[2] (1995) 377-385.
14. H.Y. Zhu and G.Q. Lu, *J. Porous Mater.* 5[5] (1998) 227-239.
15. H.Y. Zhu, Z.H. Zhu and G.Q. Lu, *J. Phys. Chem. B* 104[24] (2000) 5674-5680.
16. E.P. Barrett, L.G. Joyner and P.P. Halenda, *J. Am. Chem. Soc.* 73[1] (1951) 373-380.
17. J. Németh, I. Dékány, K. Süvegh, T. Marek, Z. Klencsár, A. Vértes and J.H. Fendler, *Langmuir* 19[9] (2003) 3762-3769.
18. K. Mogyorosi, I. Dékány and J.H. Fendler, *Langmuir* 19[7] (2003) 2938-2946.
19. J. Németh, G. Rodriguez-Gattorno, D. Diaz, A.R. Vazquez-Olmos and I. Dékány, *Langmuir* 20[7] (2004) 2855-2860.
20. S.J. Gregg and K.S.W. Sing (Eds), *Adsorption, Surface Area and Porosity*, Academic Press, London, 1982.